Application of a modified 3D U-Net convolutional neural network architecture for the inspection of aerospace components

Miroslav Yosifov[1], Patrick Weinberger[1], Bernhard Fröhler[1], Bernhard Plank[1], Johann Kastner[1], Christoph Heinzl[2,3]

[1]University of Applied Sciences Upper Austria, Wels Campus, Austria, e-mail: miroslav.yosifov@fh-wels.at

[2]University of Passau, Innstraße 43, Passau, Germany

[3]Fraunhofer Institute for Integrated Circuits IIS, Division Development Center X-ray Technology, Flugplatzstraße 75, Fürth, Germany

Abstract

This work illustrates the use of deep learning methods applied on X-ray computed tomography (XCT) datasets to segment pores and fibres in reinforced composite components from the aeronautic industry by binary semantic segmentation. We first apply data pre-processing, and then employ a modified 3D U-Net, representing a convolutional neural network. Tweaking hyper-parameters, we have reached an optimal model for our datasets. One of the models has reached 99% segmentation accuracy when testing using a Dice function. In our experiments, pores and fibres in XCT datasets of aerospace components, more specifically of glass and carbon fibre reinforced composites, were segmented and analysed. In order to compare this modified 3D U-Net architecture with segmentation methods currently used in the industry, the datasets were also input to conventional Otsu thresholding. Our results shows that modified 3D U-Net performs better than Otsu thresholding, especially on the segmentation of small pores. Modified 3D U-Net also showed reasonable prediction accuracy when testing with an optimised model which was trained with a low number of dataset both for fibre and pore segmentation.

Keywords: Deep learning, segmentation, U-Net, 3D U-Net, computed tomography, pores, composites, polymers.

1 Introduction

Deep learning has been successfully used in many different research fields such as computer vision [3], object recognition [4], medical image analysis [5], self-driving systems, and material inspection within past decades. One of the most popular deep learning methods are convolutional neural networks (CNN), which can be applied to the classification of objects and to image segmentation tasks. Segmenting pores in the specimen is a necessary step in characterising and analysing material properties in non-destructive testing. However, image segmentation and classification of objects (such as pores or fibres in material science) is still a challenging task even for material science domain experts. Even though there are numerous different segmentation available such as k-means, watershed and various thresholding techniques, there is still a lot of ongoing research to improve segmentation methods [6]. Reliable and efficient segmentation is important, especially for critical process in the material science industry. In order to come up with a robust and reliable segmentation, we used an convolutional neuronal network.

2 Related Work

Convolutional neural networks (CNN) have proven to be powerful image or volume segmentation methods. One well-know CNN for this purpose is the U-Net architecture [1], originally used to segment 2D microscopy images, and its extension to 3D [7]. A U-Net based network architecture from Isensee et al. [8] successfully reached the second and third rank in the Brain tumour segmentation challenge [9]. In recent years, many U-Net variants such as Residual U-Net [14], UNet++ [16], Dense U-Net [15] and Adversarial U-Net (i.e GAN, CGAN) [17] have been devised to segment or transform images or volumes. Detailed explanations as well as a comparison of a number of U-Net variants have been explored by Siddique et al. [18].
Impressive results with U-Net in the medical application also paved the way of using U-Net for materials science purposes. In the materials science, the accurate segmentation of pores plays an important role to analyse data or specimen quality. To improve segmentation accuracy, 3D U-Net was updated and optimised to an architecture applicable for fibre composites as presented by Yosifov [11]. To segment defect features on short glass fibres by using transfer learning and Tversky loss function applied on the challenging specimens has been introduced by Weinberger et al. [10]. It showed that transfer learning can reduce the training time and the amount of data needed for accurate segmentation.

3 Method

As reference for the training we used manually segmented data based on conventional thresholding. The data was split into smaller sub-volumes and used in our training pipeline. We evaluated the network on two different types of datasets. We also explored two different use cases from the aeronautic industry to compare the segmentation of modified 3D U-Net and Otsu thresholding which are found in the:

https://doi.org/10.58286/27728

- Segmentation of pores in a carbon fibre reinforced polymer (CFRP) part
- Segmentation of fibres in a glass fibre reinforced polymer (GFRP) part

In the following sections the Modified 3D U-Net Architecture is briefly introduced as well as the data we have been working with, the training and hyper parameters.

3.1 Modified 3D U-Net Architecture

We implemented a modified 3D U-Net network architecture [10, 11] in Python using Keras with TensorFlow as a back end. This network includes two paths respectively called contracting path (encoder) and expansive path (decoder), with a U-shaped architecture containing four encoder and decoder blocks (see Figure 1).

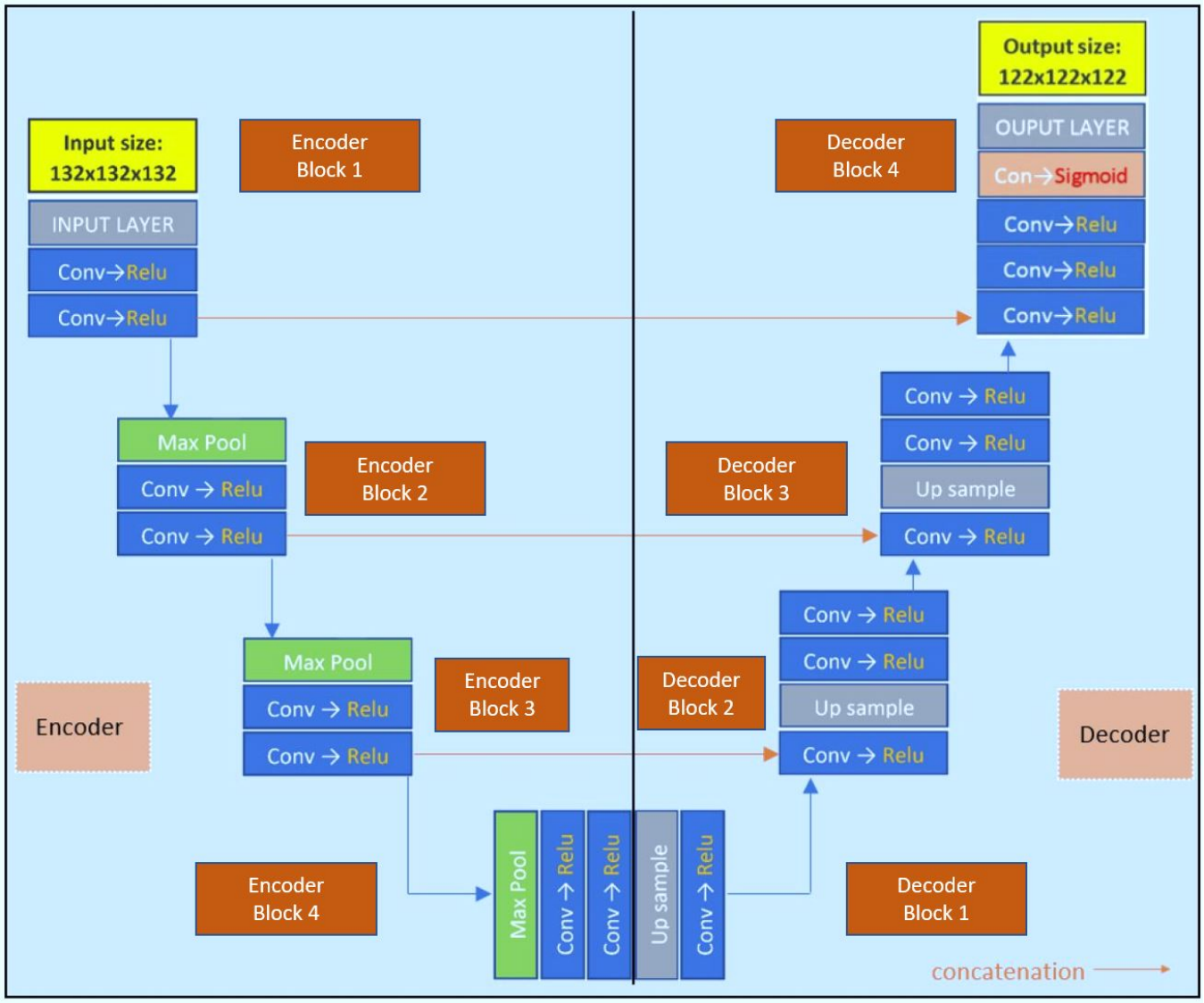

Figure 1: Architecture of the modified 3D U-Net model (Adapted from [10, 11]).

3.2 Data Characteristics

The scanning device GE Nanotom 180 NF was used to generate XCT datasets. The chosen resolution was (3.3 μm)^3 voxel size for reference scans, which were used to train the algorithm, and (10 μm)^3 for the final evaluations. Data characteristics are presented in Table 1. CFRP samples were used for pore segmentation, while GFRP samples were used for fibre segmentation.

3.3 Training and Hyperparameters

We used a similar pipeline and network architecture as in our previous publications [10, 11]. To reduce the memory consumption, the network was designed to predict sub-volumes with a size of 122x122x122 voxels. To improve the network performance, an

Table 1: SAMPLE MODALITY

Sample No	Resolution	Size	Data usage
CFRP Sample 1	3.3 μm	$1220 \times 854 \times 976$	Training
CFRP Sample 2	3.3 μm	$1220 \times 854 \times 976$	Testing
CFRP Sample 3	10 μm	$366 \times 244 \times 244$	Testing
GFRP Sample 1	2.7 μm	$1098 \times 976 \times 1098$	Training
GFRP Sample 2	2.7 μm	$610 \times 610 \times 610$	Testing
GFRP Sample 3	3 μm	$632 \times 632 \times 632$	Testing

overlapping tile approach [1] was used, where the input size with 132x132x132 is bigger than the predict size of 122x122x122 (i.e., 5 voxels overlap). The general pre-processing pipeline contained the following steps also shown in Figure 2.

- Normalising the input data
- Adding mirror-padding (5 voxels)
- Splitting the CT scan and labelled volume into sub-volumes with an overlapping of 5 voxels in every direction (hence a 132x132x132 input and 122x122x122 output volume size)

The major change to our previous publication [10] was the loss function: In this paper we used Dice loss instead of focal Tversky loss. For our two use cases was the imbalanced between the classes were not too high, therefore Dice loss which is based on the dice coefficient[19] was used. The pre-processing pipeline was implemented in Python. For training, we used only the sub-volumes of CFRP Sample 1 and GFRP Sample 1 individually. In the result evaluation, only unseen data was used (for pore segmentation: CFRP Sample 2 and 3, for fibre segmentation GFRP Sample 2 and 3). The datasets for segmentations have been split into two parts: 80% of the sub-volumes for training and 20% for testing.

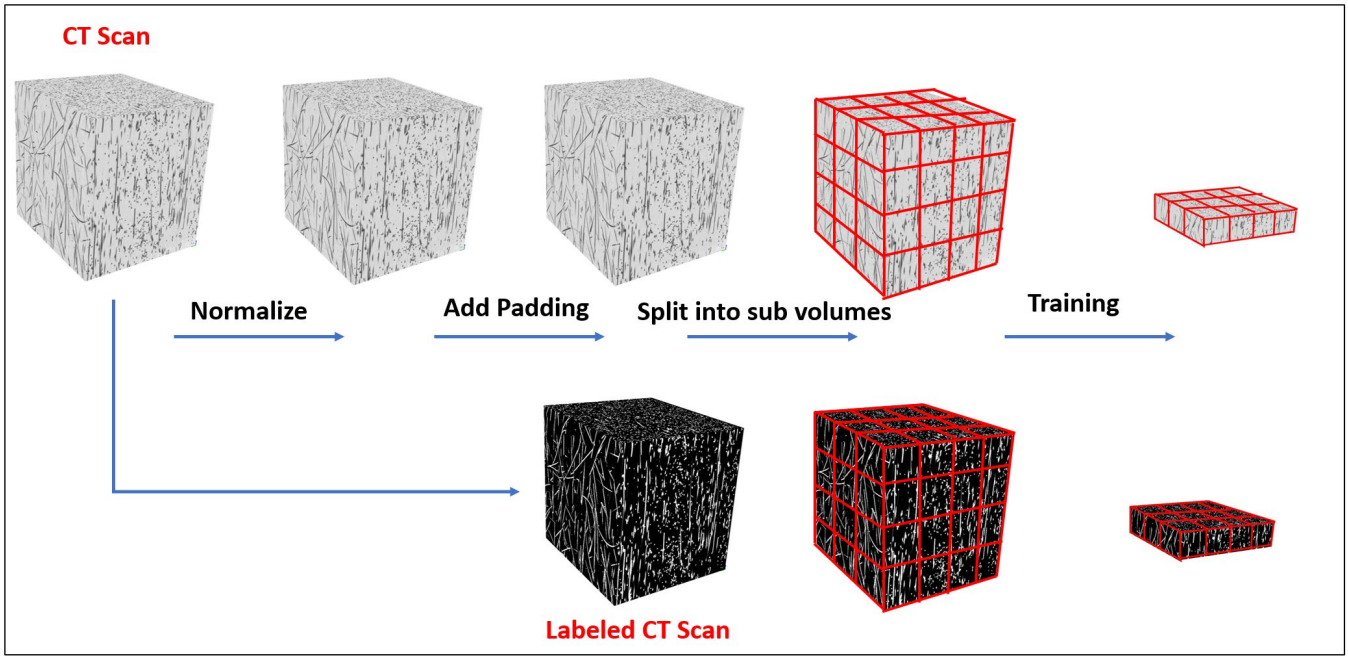

Figure 2: Illustration of our training pipeline

4 Result Evaluation and Discussion

For both use cases the modified 3D U-Net network showed a reasonable performance after around 1200 training steps with a batch size of 3. In some areas, our network performed even better than Otsu thresholding. The network also performed well on a dataset with a different resolution (10 μm) it was not trained on. In this workflow, we measure quality by visual inspection. As mentioned in subsection 3.3, results were generated only on the unseen data. For the training process, firstly CFRP sample 1 was used, then the training model was applied on CFRP sample 2 and 3. Similarly, GFRP sample 1 was used for training and GFRP sample 2 and 3 used in testing process.

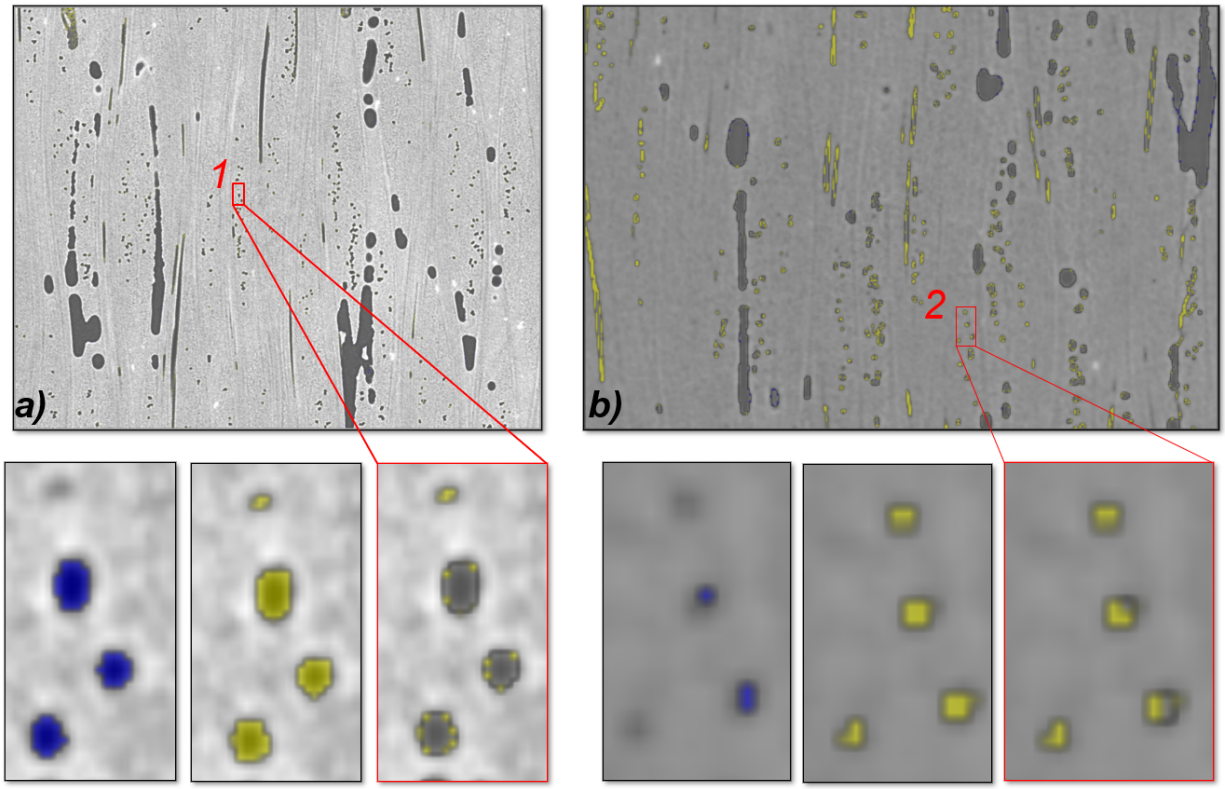

Figure 3: 2D XCT slices of CFRP input images. a) and b) show 3.3 μm and 10 μm resolution images, respectively, with Otsu segmentation (blue) and neural network prediction (yellow), as well as overlaid (dark grey where they agree) on the specimen. The enlarged images of detail regions 1 and 2 below show three separate views for Otsu segmentation, neural network prediction and their differences (from left to right).

4.1 Pore Segmentation in CFRP

The detail region 1 in Figure 3a) shows quite similar results for Otsu based thresholding segmentation and the prediction of the of the network. It seems, that the network is segmenting more than the threshold based algorithm. Especially, detail region 2 in b) shows the benefits of a deep neuronal network, because here it was able to segment much more pores. This finding is explained by the fact that the network is not only limited to make decisions based on a fixed threshold. It can also take into account the shape and gradients. For Otsu thresholding however, the contrast is not high enough to segment also these small pores in lower resolution images.

4.2 Fibre Segmentation in GFRP

The results for the fibres in figure 4 detail b) (2.7 μm) show that here Otsu thresholding has performed similarly or better than the 3D U-Net model. For the detail c) (3 μm) where the contrast between fibre and background is higher, the CNN has segmented more than the threshold based algorithm.

5 Performance

The training with an Nvidia Quadro RTX6000 for the pore and also for the fibre task has taken approximately one hour. The inference of a volume with a size of $1220 \times 854 \times 976$ voxels in open_iA [2] with the same GPU takes around 2 minutes, which also includes the preprocessing steps as indicated (i.e., normalisation and splitting into sub-volumes). In comparison, the segmentation with Otsu using open_iA takes 5 seconds, for a volume with the same size, only using 1 Core of the CPU.

6 Conclusion

The modified 3D U-Net architecture shows reasonable performance on different resolutions, even with a limited set of reference data. If we compare the results between Otsu thresholding and our approach by visual inspection, the modified 3D U-Net model performs better than a threshold based algorithm in several areas, especially for the detection of small pores. The modified 3D U-Net also performs reasonably well on untrained datasets and different resolutions. We extended open_iA to use a trained 3D U-Net for segmentation. With the overlapping tile approach, it is possible to apply it on bigger volumes (such as XCT scans with

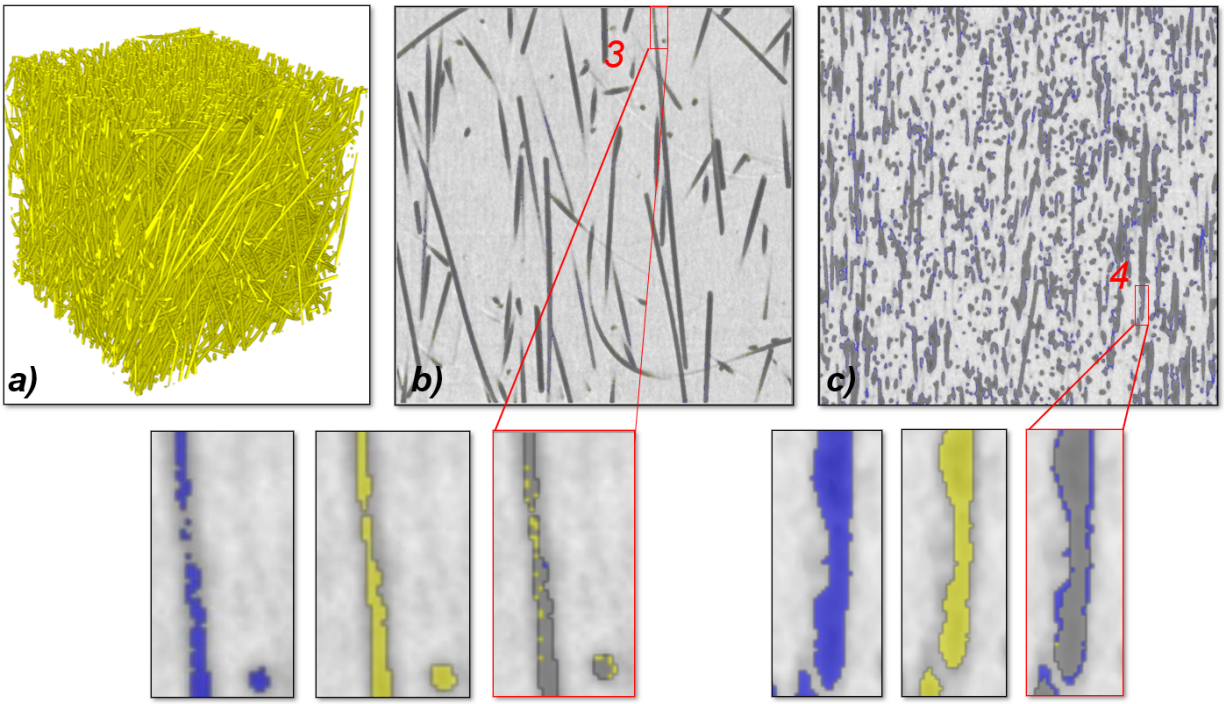

Figure 4: 3D view of modified 3D U-Net segmentation (a) and 2D XCT slices of GFRP input images. b) and c) show 2.7 μm and 3 μm resolution images respectively, with Otsu segmentation (blue) and neural network prediction (yellow), as well as overlaid (dark grey where they agree) on specimen. The enlarged images of detail regions 3 and 4 below show three separate views for Otsu segmentation, neural network prediction and their differences (from left to right).

$1000 \times 1000 \times 1000$ voxels in size or larger). Our findings show that the quality of the ground truth data (i.e., binary masks) for the training plays an essential role in training the neural network regarding efficient predictions.
One of the biggest challenges is always to find the balance between the segmentation quality and the effort to perform the segmentation. The modified 3D U-Net delivers slightly better results than Otsu thresholding. In our case, there is a high contrast between pores/fibres and background, so Otsu provides nearly as good results as the modified 3D U-Net. When comparing the execution times, Otsu is however much faster. In contrast, in our previous publication [10] we have shown that CNNs also perform well on tasks for which threshold-based algorithms cannot deliver reasonable results.
For future work, we will focus more on datasets that are difficult to impossible to segment using conventional techniques. For those, we intend to improve our reference segmentation using a labelling software where a human expert manually segments XCT images in 2D and 3D. In the next generation of our pipeline, it is planed to use image augmentation to improve the generalisation, in combination with a human in the loop approach to reduce the manual effort. Human in the loop means here that the network makes a prediction, which is then corrected by a human expert, until the quality of the prediction reaches a predefined threshold. Another important point is the use of additional measures to quantify the results of the prediction better, in similar directions as Yosifov et al. [12] or Weissenböck et al. [13]. Especially the shape and volume of the pores are important for aerospace components.

Acknowledgements
The research leading to these results has received funding from the Austrian Research Promotion Agency (FFG) within the program line “TAKE OFF” under the grant number 874540 “BeyondInspection”. The research leading to these results has also received funding by the government of Upper Austria within the project “X-PRO”, as well as “XPlain”, grant no. 895981. This research was also co-financed by the European Union H2020-MSCA-ITN-2020 under grant agreement no. 956172 (xCTing).

References

[1] O. Ronneberger, P. Fischer, T. Brox, U-Net: Convolutional Networks for Biomedical Image Segmentation, in: Proceedings of the International Conference on Medical Image Computing and Computer-Assisted Intervention (MICCAI), Munich, Germany (2015) 234–241. doi: 10.1007/978-3-319-24574-4_28.
[2] B. Fröhler, J. Weissenböck, M. Schiwarth, J. Kastner, C. Heinzl, open_iA: A tool for processing and visual analysis of industrial computed tomography datasets, Journal of Open Source Software 4 (35) (2019) 1185. doi: 10.21105/joss.01185.

[3] D. Ciresan, U. Meier, J. Schmidhuber, Multi-column deep neural networks for image classification, In Proc. IEEE Conf. Computer Vision and Pattern Recognition (2012) 3642–3649. doi: 10.1109/cvpr.2012.6248110.
[4] J. Ba, V. Mnih, K. Kavukcuoglu, Multiple object recognition with visual attention, 2014. arXiv: 1412.7755.
[5] J. Ker, L. Wang, J. Rao, T. Lim, Deep Learning Applications in Medical Image Analysis, in: IEEE Access 6 9375–9389 (2018).
[6] J. Kastner, B. Plank, D. Salaberger, J. Sekelja, Defect and porosity determination of fibre reinforced polymers by X-ray Computed Tomography, in: 2nd Int. Symposium on NDT in Aerospace. Hamburg, Germany, 2010.
[7] Ö. Çiçek, A. Abdulkadir, S. S. Lienkamp, T. Brox, O. Ronneberger, 3D U-Net: Learning Dense Volumetric Segmentation from Sparse Annotation, In Proc. Int. Conf. Medical Image Computing and Computer-Assisted Intervention (MICCAI), Athens, Greece, 2016, 424–432, doi: 10.1007/978-3-319-46723-8_49.
[8] F. Isensee, P. Kickingereder, W. Wick, M. Bendszus, K.H. Maier-Hein, Brain Tumor Segmentation and Radiomics Survival Prediction: Contribution to the BRATS 2017 Challenge, in: 3rd Int. Workshop on Brainlesion (BrainLes), MICCAI 2017, 287–297, doi: 10.1007/978-3-319-75238-9_25.
[9] S. Bakas et al., Identifying the Best Machine Learning Algorithms for Brain Tumor Segmentation, Progression Assessment, and Overall Survival Prediction in the BRATS Challenge, 2018, arXiv: 1811.02629.
[10] P. Weinberger, J. Maurer, B. Fröhler, J. Kastner, C. Heinzl, Faster Training of Deep Convolutional Neural Networks for Material Science through Transfer Learning, in: International Symposium on NDT in Aerospace, 2020, Williamsburg, Virgina, United States.
[11] M. Yosifov, Extraction and Quantification of Features in XCT Datasets of Fibre Reinforced Polymers Using Machine Learning Techniques(Master's thesis). Umeå University, Department of Computing Science.
[12] M. Yosifov, M. Reiter, S. Heupl, C. Gusenbauer, B. Fröhler, R. Fernández-Gutiérrez, J. De Beenhouwer, J. Sijbers, J. Kastner, C. Heinzl, Probability of detection applied to X-ray inspection using numerical simulations, in: Nondestructive Testing and Evaluation. 37, 5, p. 536–551, doi: 10.1080/10589759.2022.2071892.
[13] J. Weissenböck, A. Amirkhanov, E. Gröller, J. Kastner, C. Heinzl, PorosityAnalyzer: Visual analysis and evaluation of segmentation pipelines to determine the porosity in fiber-reinforced polymers. In: IEEE Conference on Visual Analytics Science and Technology (VAST), 2016, p. 101–110. doi: 10.1109/VAST.2016.7883516.
[14] K. He, X. Zhang, S. Ren, J. Sun, Deep Residual Learning for Image Recognition, in: IEEE Conference on Computer Vision and Pattern Recognition (CVPR), Las Vegas, USA (2016) 770–778, doi: 10.1109/CVPR.2016.90.
[15] G. Huang, Z. Liu, L. Van Der Maaten, K.Q. Weinberger, Densely Connected Convolutional Networks. in: IEEE Conference on Computer Vision and Pattern Recognition (CVPR), Honolulu, USA (2017) 4700–4708, doi: 10.1109/CVPR.2017.243.
[16] Z. Zhou, M.M. Rahman Siddiquee, N. Tajbakhsh, J. Liang, UNet++: A Nested U-Net Architecture for Medical Image Segmentation. In: Deep Learning in Medical Image Analysis and Multimodal Learning for Clinical Decision Support. DLMIA ML-CDS (2018). Lecture Notes in Computer Science (11045), Springer, Cham, doi: 10.1007/978-3-030-00889-5_1.
[17] M. Mirza, S. Osindero, Conditional generative adversarial nets (2014), arXiv: 1411.1784.
[18] N. Siddique, S. Paheding, C.P. Elkin, V. Devabhaktuni, U-Net and Its Variants for Medical Image Segmentation: A Review of Theory and Applications, in: IEEE Access 9 (2021) 82031–82057, doi: 10.1109/ACCESS.2021.3086020.
[19] A. Sørensen, method of establishing groups of equal amplitude in plant sociology based on similarity of species and its application to analyses of the vegetation on danish commons, Kongelige Danske Videnskabernes Selskab, Biologiske Skrifter (1948) 1–34.